Journal of Photochemistry and Photobiology A: Chemistry 221 (2011) 58–63

Contents lists available at ScienceDirect

Journal of Photochemistry and Photobiology A: Chemistry

journal homepage: www.elsevier.com/locate/jphotochem

Peroxy ethoxyformyl nitrate, $CH_3CH_2OC(O)OONO_2$. Spectroscopic and thermal characterization

Adriana G. Bossolasco, Fabio E. Malanca*, Gustavo A. Argüello

INFIQC, Departamento de Fisicoquímica, Facultad de Ciencias Químicas, Universidad Nacional de Córdoba, Ciudad Universitaria, 5000 Córdoba, Argentina

ARTICLE INFO

Article history:
Received 17 September 2010
Received in revised form 20 April 2011
Accepted 24 April 2011
Available online 30 April 2011

Keywords:
Peroxynitrates
Absorption cross-sections
Peroxyacyl nitrates
Peroxy ethoxyformyl nitrate
Thermal stability

ABSTRACT

Synthesis of $CH_3CH_2OC(O)OONO_2$ was carried out from the photolysis of a mixture of ethyl formate ($CH_3CH_2OC(O)H$), Cl_2, NO_2, and O_2 at 253 K using UV radiation. It was characterized by IR, UV spectroscopy, and mass spectrometry. Thermal decomposition was studied between 279 and 301 K, at total pressures of 1 atm. The pressure dependence of the reaction rate constant was studied at 298 K from 7 to 1000 mbar. The activation energy was determined at a total pressure of 1 atm, ensuring that kinetic studies were performed in the high pressure limit. The DFT method [B3LYP/6.31++G(d,p)] was used to identify the most stable rotamer as well as its geometric parameters and energetics.

At room temperature, $CH_3CH_2OC(O)OONO_2$ is stable for several days in the gas state, as revealed by its measured lifetime. The atmospheric implications of this finding are discussed.

1. Introduction

The study of peroxyacyl nitrates ($RC(O)OONO_2$) is relevant because of their role as reservoir species in the atmosphere [1–3]. As it is known, their stability increases when temperature decreases, leading to atmospheric lifetimes of days at the lower troposphere and years near to tropopause [4–6]. Only few peroxyacyl nitrates have been detected and measured in the atmosphere, among which we can cite peroxyacetyl (PAN), propionyl (PPN), and benzoyl (PBzN) nitrates [7–9]. These molecules are formed in the atmospheric degradation of volatile organic compounds emitted to the atmosphere [3,10,11].

Several peroxynitrates were observed in laboratory studies as products of the oxidation mechanism of hydrogenated and fluorinated compounds in the presence of NO_2 [1,5,12–18]. However, only few peroxynitrates were synthesized and fully characterized [11,17–21].

Recent laboratory studies have shown that the atmospheric oxidation of ethyl formate, an organic compound extensively used as a fumigant and pesticide, leads to the formation of peroxy ethoxyformyl nitrate ($CH_3CH_2OC(O)OONO_2$, PEFN) [13]. The reaction mechanism involves the H-atom abstraction on the carbonyl group

$$CH_3CH_2OC(O)H + Cl^\bullet \rightarrow CH_3CH_2OCO^\bullet + HCl \quad (1)$$

followed by the reaction of the radical formed with O_2 to yield a peroxy radical

$$CH_3CH_2OCO^\bullet + O_2 \rightarrow CH_3CH_2OC(O)OO^\bullet \quad (2)$$

and the subsequent reaction with NO_2

$$CH_3CH_2OC(O)OO^\bullet + NO_2 \rightarrow CH_3CH_2OC(O)OONO_2 \quad (3)$$

This mechanism was proposed by Malanca et al. [13], who determined that about 30% of ethyl formate is converted into PEFN. The possible existence of this molecule in the atmosphere makes a complete knowledge of its chemical and physical properties necessary.

In this work we present some previously unreported characteristics of PEFN, which were found by studying its ultraviolet and infrared absorption cross-sections, mass spectra, thermal behavior and structural details. The atmospheric lifetimes of this molecule were estimated from UV absorption cross-sections and thermal decomposition rate constants.

2. Experimental

2.1. Photochemical synthesis of $CH_3CH_2OC(O)OONO_2$

Volatile materials were manipulated in a glass vacuum line equipped with two capacitance pressure gauges (0–760 Torr, MKS Baratron; 0–70 mbar, Bell and Howell). Peroxy ethoxyformyl nitrate (PEFN, $CH_3CH_2OC(O)OONO_2$) was synthesized by photolysis of mixtures containing $CH_3CH_2OC(O)H$ (7.0 mbar)/Cl_2

* Corresponding author. Tel.: +54 351 433 4169; fax: +54 351 433 4188.
E-mail address: fmalanca@fcq.unc.edu.ar (F.E. Malanca).

1010-6030/$ – see front matter © 2011 Elsevier B.V. All rights reserved.
doi:10.1016/j.jphotochem.2011.04.024

(2.5 mbar)/NO_2 (4.0 mbar)/O_2 (1000 mbar), using black lamps ($\lambda > 360$ nm) as reported in Ref. [13]. Improvements on the original method will be briefly discussed below.

The photolysis was carried out in a 5 L glass flask maintained at −20 °C to decrease thermal decomposition of PEFN. This greatly improved the yield of the product as compared to the room temperature method described in Ref. [13]. The progress of the synthesis was checked every 30 min through infrared spectroscopy and was stopped when NO_2 had almost disappeared. Approximately 1% of the flask content was transferred each time to a 250 mL IR cell (optical path 23.0 cm, KBr windows) placed in the sample compartment of the IFS 66v FTIR Spectrometer. After photolysis, the mixture was collected by slowly passing it through three traps kept at −186 °C to remove excess O_2.

The whole procedure was carried out five times and the crude of the reaction was collected to obtain meaningful quantities. The resulting mixture contained ClNO (nitrosyl chloride), $ClNO_2$ (nitryl chloride), HCl, HC(O)OH (formic acid), $CH_3C(O)OONO_2$ (peroxy acetyl nitrate, PAN), $CH_3CH_2ONO_2$ (ethyl nitrate), $CH_3CH_2OC(O)OONO_2$ as well as $CH_3CH_2OC(O)H$ (EF, ethyl formate) and NO_2. It was trap-to-trap distilled: first, between −100 and −186 °C to eliminate the more volatile fraction containing ClNO, $ClNO_2$, CO_2, and HCl. Then, subsequent distillations were carried out between −75 °C and −120 °C which mainly allowed the extraction of EF and $C_2H_5ONO_2$. The more volatile fraction containing PEFN, PAN, and HC(O)OH as well as the remnants of EF was treated between −60/−50 °C and −120 °C, leading to the elimination of PAN, EF, and a fraction of formic acid. The resulting sample contained mainly PEFN and a small quantity of formic acid (Fig. 1) which it was not possible to separate, probably because of their similar vapor pressures. The addition of sodium bicarbonate to neutralize formic acid led readily to its elimination, but it also resulted in some PEFN being destroyed, probably as a consequence of heterogeneous reactions. However, trace quantities of formic acid do not interfere with PEFN characterization (see Fig. 1).

2.2. IR and UV spectroscopy. Mass spectrometry

Gas-phase infrared spectra were recorded at room temperature, at a resolution of 2 cm^{-1} in the range 4000–400 cm^{-1}, using the IR cell described above. The spectrum of the pure sample is plotted in Fig. 1, where the calibration curve is shown at 1224 cm^{-1}. The corresponding cross-sections as well as the tentative assignment of its vibrations are collected in Table 1.

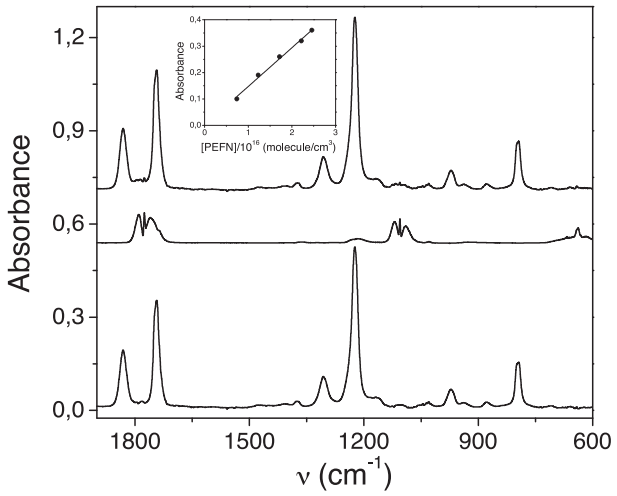

Fig. 1. Infrared spectrum of PEFN. The upper trace shows the spectrum of a sample containing PEFN and HC(O)OH. Subsequent traces correspond to infrared spectra of pure samples of HC(O)OH and PEFN, respectively. The inset shows the calibration curve of PEFN at 1224 cm^{-1}.

UV spectra were obtained with a Hewlett–Packard 8453 Agilent Spectrophotometer with a diode array detector. They were recorded using a UV glass cell (optical path 10.0 cm).

Absorption cross-sections (σ) were determined according to Eq. (1)

$$\sigma(\mathrm{cm^2\ \ molecule^{-1}}) = 31.79 \times 10^{-20}$$
$$(\mathrm{mbar\ \ cm^3\ \ molecule^{-1}\ \ K^{-1}}) \times T \times A \times (p \times d)^{-1}$$

where T denotes the temperature (K), A is the absorbance, p is the pressure (mbar) and d denotes the optical path (cm). The pressure ranges used for the determination of infrared and UV spectra were 0.3–1.0 (Fig. 1) and 3.0–12.0 mbar, respectively, where the Beer–Lambert law can be used without deviations (see the inset in Fig. 1 for IR measurements).

Mass spectra were obtained in the electron impact mode (EI) with a 70 eV ionization energy in a FINNIGAN 3300 F-100 Spectrometer.

Table 1
Observed and calculated vibrational wavenumbers of PEFN, and their corresponding relative intensities. Bands with intensity higher than 1% have been included.

Vibrational data and assignment				
Experimental IR gas (cm^{-1})	Calculated syn–syn	Relative intensity (%)		Assignment/approximate description of modes
		Experimental	Calculated	
	3145		2.9	
	3128		1.8	
	3078		1.3	
	3053		1.3	
1831	1868	33	28.8	Stretching C=O
1744	1821	69	46.3	Antisymmetric stretch O–N–O
	1520		1.0	
	1435		1.3	
1308	1365	17	14.9	Symmetric stretch O–N–O
1224	1255	100	100	Antisymmetric stretch O–C–O
	1136		1.6	
973	1004	12	13.7	Stretching O–O
	959		4.5	
	889		3.0	
796	798	24	20.4	Scissoring O–N–O
	767		1.7	
	710		1.2	
	522		3.0	

2.3. Kinetics and thermal decomposition as a function of T

Thermal stability was determined by monitoring the temporal variation of the infrared spectra of PEFN in the presence of 1.0 mbar of NO and enough nitrogen to reach 1 atm, and varying the temperatures between 301 and 279 K. NO was added to the sample to irreversibly trap the peroxy radicals formed from the decomposition of PEFN.

Additionally, the pressure dependence of the rate constant for decomposition was studied between 7 and 1000 mbar to obtain the high pressure limit of the unimolecular dissociation.

The disappearance of PEFN was tracked using the IR absorption band at 1224 cm^{-1} since this is the only one presenting the highest cross-section. The data were analyzed according to a first-order rate law. For each temperature, the decay was fitted by a linear regression and the value associated with the rate constant, together with its statistical uncertainty (as a vertical bar), was plotted in the Arrhenius form.

3. Materials

Commercially available samples of ethyl formate (Riedel-de-Haën), NO (AGA), and O_2 (AGA) were used. Oxygen was condensed while flowing at atmospheric pressure through a trap immersed in liquid air, and then it was pumped under vacuum several times. NO_2 was prepared by adding O_2 to NO, and it was then purified. Cl_2 was synthesized by direct reaction between HCl and $KMnO_4$ in a nitrogen flow, it was collected in a trap immersed in liquid air and distilled.

4. Results and discussion

4.1. Geometric parameters

Quantum chemical calculations were performed with the Gaussian 03 program suite [22]. Scans of the potential energy surface, optimizations, and calculations of the vibrational frequencies of possible conformers of PEFN were carried out applying Density Functional Theory (B3LYP) methods with 6-311++G(d,p) basis sets. The superiority of DFT methods over conventional Hartree–Fock ones for the study of oxygenated systems has been demonstrated [23–25]. The potential energy curve for the internal rotation around the O1–C3 single bond was derived by structure optimization at fixed dihedral angles φ(C2–O1–C3–O2) from 0° to 180°. The curve obtained (Fig. 2) shows two minima corresponding to the stable conformers syn–syn and syn–anti, respectively. The conformers were named according to the following criteria: (a) the position of the C=O bond with respect to the O–O bond defines the first term, whether syn or anti; and (b) the position of the CH_3CH_2–O bond with respect to the C=O bond defines the second syn–anti term. For both conformers, the O–C–O–O skeleton has a gauche configuration. At this level of theory, the syn–syn conformer is the most stable by 3.7 kcal mol^{-1} and the energy barrier is 8.7 kcal mol^{-1} (Fig. 2), in agreement with the range of values typical of this kind of rotations [26].

Picture 1 shows the structure of the syn–syn conformer, whose geometric parameters are presented in Table 2. The most relevant features in the structure of the peroxides are the dihedral angle around the O–O bond as well as its length. Such angle is around ≤90 for peroxides with two strongly withdrawing substituents (e.g., Cl, F) or with sp^2-hybridized substituents (e.g., RC(O), NO_2). The calculated value for $C_2H_5OC(O)OONO_2$ φ(C–O–O–N) is 87.8°, similar to the value reported by Badenes and Cobos for $C_2H_5C(O)OONO_2$ (85.9°) [26]. The O–O bond distance (1.40 Å) is in agreement with those reported for $C_2H_5C(O)OONO_2$ and other peroxides [27].

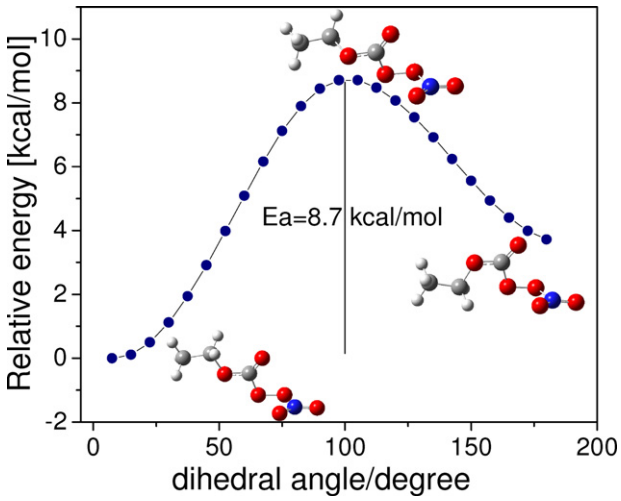

Fig. 2. Potential energy barrier for internal rotation around the C3–O3 bond of PEFN calculated at the B3LYP/6-311++G(d,p) level.

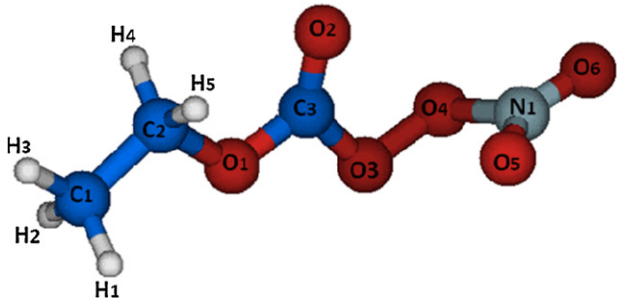

Picture 1. Calculated structure for the most stable syn–syn $CH_3CH_2OC(O)OONO_2$ conformer.

4.2. Spectroscopic characterization

The results in Table 1 complement the information on the infrared spectrum of PEFN reported in our previous work (Ref. [13]), where only the infrared bands were presented.

Table 3 lists the absorption cross-sections for PPN ($C_2H_5C(O)OONO_2$, peroxypropionyl nitrate), PnBN ($CH_3(CH_2)_2C(O)OONO_2$, peroxy-*n*-butyryl nitrate), PnVN ($CH_3(CH_2)_3C(O)OONO_2$, peroxy-*n*-valeryl nitrate), PAN ($CH_3C(O)OONO_2$, peroxyacetyl nitrate) [28], and PEFN ($C_2H_5OC(O)OONO_2$, peroxy ethoxyformyl nitrate) of the most intense absorptions at around 790, 1030–1040, 1300, 1740, and

Table 2
Calculated geometric parameters of the most stable conformer.

Geometric parameters			
Distances (Å)		Angles (°)	
C1–H(1,2,3)	1.09	H3–C1–C2	109.14
C2–H(4,5)	1.09	H2–C1–C2	111.06
C1–C2	1.51	H1–C1–C2	111.12
C2–O1	1.46	C1–C2–O1	107.22
O1–C3	1.32	H(4,5)–C2–O1	107.98
C_3–O_2	1.20	C2–O1–C3	115.61
C3–O3	1.40	O1–C3–O2	129.76
O3–O4	1.40	O2–C3–O3	125.38
O_4–N_1	1.52	C3–O3–O4	109.91
N1–O5	1.19	O4–N1–O5	116.79
N1–O_6	1.19	O4–N1–O6	109.34
		O5–N1–O6	133.86
		5 (C–O–O–N)	87.8
		5 (O–C–O–O)	−6.79

Table 3
Absorption cross-sections of PAN, PPN, PnBN, PnVN, and PEFN. The bracketed values correspond to uncertainties.

$\sigma \times 10^{19}$ (cm^2 $molecule^{-1}$)					
Wavenumber (cm^{-1})	PAN[a]	PPN[b]	PnBN[b]	PnVN[b]	PEFN[c]
794	9.5 (0.2)				
796		9.04 (0.09)	5.40 (0.09)	7.3(0.1)	3.2 (0.3)
973					1.5(0.1)
1037			2.59 (0.05)		
1044		2.7 (0.09)			
1050				4.40 (0.03)	
1163	12.1 (0.3)				
1224					13.4(0.9)
1300			5.8(0.1)		
1301		10.1 (0.2)			
1302	9.2 (0.2)				
1304				7.8 (0.2)	
1308					2.3 (0.5)
1738				2.0 (0.3)	
1738		20.6 (0.2)			
1741	23.9 (0.6)				
1741			14.5(0.2)		
1744					9.3 (0.5)
1831					4.4 (0.4)
1832				4.66 (0.04)	
1834			6.63 (0.06)		
1835		5.97 (0.07)			
1842	7.4 (0.3)				

[a] Determined by Allen et al. [28].
[b] Determined by Monedero et al. [29].
[c] Values obtained in this work.

1830 cm^{-1} which correspond to NO_2 scissors, NO_2 symmetric stretch, NO_2 asymmetric stretch, and CO stretching [29]. As it can be seen, the infrared absorption cross-sections of PEFN are similar to those for the other peroxyacyl nitrates, which range between 0.2 and 2.0 $\times 10^{-18}$ cm^2 $molecule^{-1}$, but the most intense band at 1224 cm^{-1} ($\sigma = 13.4 \times 10^{-19}$ cm^2 $molecule^{-1}$), presents a distinguishing feature of PEFN, i.e., the antisymmetric stretching O–C–O, which is absent in all the other nitrates.

Table 4 shows the UV absorption cross-sections measured at intervals of 2 nm with their standard deviations (bracketed values). They were obtained as an average of independent measurements of the neat substance at different pressures. According to the maximum pressure of PEFN used to determine the UV spectrum (12 mbar), an absorbance value of 0.005 (our limit of confidence) corresponds to 5×10^{-22} cm^2 $molecule^{-1}$. This value is reported as the error for wavelengths greater than 300 nm.

Fig. 3 depicts the UV spectra of PEFN and of other selected peroxyacyl nitrates: $CH_3CH_2C(O)OONO_2$, $CH_3CH_2OC(O)OONO_2$, $CF_3C(O)OONO_2$, and $CF_3OC(O)OONO_2$. As it can be seen, the spectrum of PEFN has many similarities with the other peroxynitrates, namely being non-structured and having higher absorption cross-sections at shorter wavelengths. Analyses of the spectra suggest that on account of their structure the presence of an O-atom in the alkyl chain of the molecule leads to a decrease in the absorption cross-section. This trend is observed for both fluorinated and hydrogenated compounds, like those shown in Fig. 3.

The fragmentation pattern obtained in the electron impact mode shows the presence of the peaks at *m/z* 27, 28, 29,30,44, 45, 46, and 73, which correspond to $C_2H_3^+$ (25), CO^+ (37), $C_2H_5^+$ (14), NO^+ (30), CO_2^+ (100), $C_2H_5O^+$ (5), NO_2^+ (12) and $C_2H_5OCO^+$ (0.4), respectively, in agreement with the identity of the molecule.

5. Thermal decomposition

The study of the thermal decomposition of PEFN was carried out by adding NO to the sample to irreversibly trap the peroxy radicals formed (reaction (4))

$$CH_3CH_2OC(O)OONO_2 \rightarrow CH_3CH_2OC(O)OO^\bullet + NO_2 \quad (3')$$

$$CH_3CH_2OC(O)OO^\bullet + NO \rightarrow CH_3CH_2OC(O)O^\bullet + NO_2 \quad (4)$$

followed by decomposition of acyl–oxy radicals and a subsequent reaction with NO to form ethyl nitrite (CH_3CH_2ONO)

$$CH_3CH_2OC(O)O^\bullet \rightarrow CH_3CH_2O^\bullet + CO_2 \quad (5)$$

Table 4
UV absorption cross-sections of PEFN at 298 K. The bracketed values correspond to uncertainties.

Wavelength (nm)	$\sigma \times 10^{20}$ (cm^2 $molecule^{-1}$)	Wavelength (nm)	$\sigma \times 10^{20}$ (cm^2 $molecule^{-1}$)
200	276 (8)	258	1.8 (0.2)
202	245 (8)	260	1.6 (0.2)
204	212 (8)	262	1.4 (0.1)
206	179 (8)	264	1.3 (0.1)
208	151 (8)	266	1.1 (0.1)
210	123 (7)	268	0.95 (0.09)
212	100 (7)	270	0.85 (0.09)
214	81 (7)	272	0.77 (0.09)
216	65 (6)	274	0.65 (0.08)
218	52 (5)	276	0.62 (0.08)
220	42 (4)	278	0.56 (0.08)
222	33 (3)	280	0.52 (0.08)
224	27 (3)	282	0.46 (0.08)
226	21 (2)	284	0.43 (0.08)
228	17 (1)	286	0.35 (0.07)
230	13 (1)	288	0.32 (0.07)
232	10.8 (0.9)	290	0.29 (0.07)
234	8.8 (0.9)	292	0.26 (0.07)
236	7.4 (0.8)	294	0.24 (0.07)
238	5.9 (0.7)	296	0.21 (0.06)
240	5.1 (0.6)	298	0.19 (0.06)
242	4.3 (0.5)	300	0.17 (0.06)
244	3.9 (0.4)	302	0.16 (0.05)
246	3.4 (0.3)	304	0.14 (0.05)
248	3.0 (0.3)	306	0.13 (0.05)
250	2.7 (0.3)	308	0.12 (0.05)
252	2.5 (0.2)	310	0.11 (0.05)
254	2.2 (0.2)	312	0.09 (0.05)
256	2.0 (0.2)	314	0.08 (0.05)

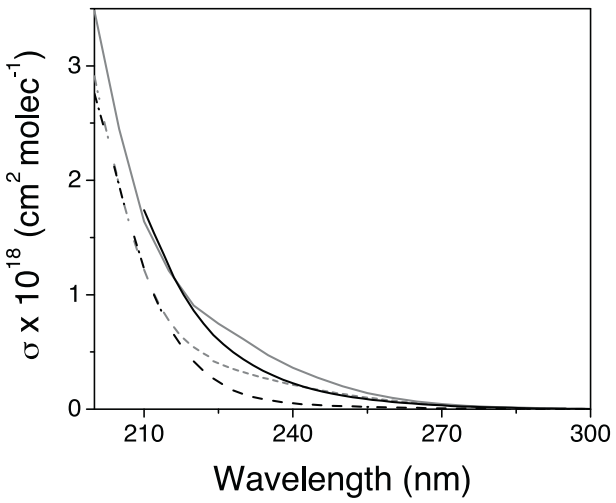

Fig. 3. UV spectra of peroxyacyl nitrates, $RC(O)OONO_2$. R: CH_3CH_2O (black dotted line), CH_3CH_2 (black solid line) [11], CF_3O (gray dotted line) [16], and CF_3 (gray solid line) [18].

$$CH_3CH_2O^{\bullet} + NO \rightarrow CH_3CH_2ONO \quad (6)$$

Typical concentrations were 2.0 mbar of PEFN, and 1.0 mbar of NO. In order to establish whether the rate constant of decomposition is pressure dependent, a series of experimental runs were performed at 294.6 K and at different total pressures. The results showed that the rate constant at pressures of 1000, 300, 100, 70, 30.0, and 7.0 mbar were 8.5 ± 0.1, 8.54 ± 0.08, 8.41 ± 0.09, 8.2 ± 0.1, 7.3 ± 0.1, and $6.0 \pm 0.1 \times 10^{-4}$ s^{-1}, respectively. The observed pressure dependence is similar to that reported by Manetti et al. in their study on thermal decomposition of $CF_3OC(O)OONO_2$ [4]. For this reason, all kinetic determinations were carried out in the high pressure limit.

Fig. 4 shows the temporal variation of the 1224 cm^{-1} absorption band at different temperatures (301–279 K) and at a total pressure of 1 atm. From every slope, a particular value of k_{-3} has been derived.

The temperature dependence of k_{-3} (s^{-1}) can be described by the Arrhenius equation

$$\ln\ k_{-3} = \ln\ A - \frac{E_a}{RT}$$

where $\ln A = (37 \pm 3)$ and $E_a = (108 \pm 5)$ kJ mol^{-1}, and has been plotted as an inset in Fig. 4.

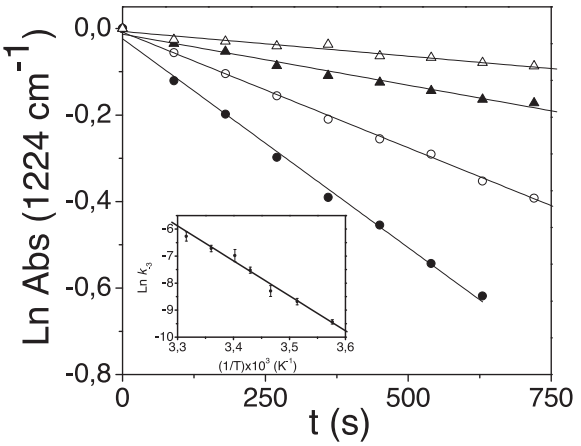

Fig. 4. First-order decay plots at: △ 279.6, ▲ 288.5, ◯ 293.9, and ● 301.2 K. The inset shows the Arrhenius plot for k_{-3}.

Table 5
Kinetic parameters for the thermal decomposition of peroxynitrates. The rate constant for PEFN was calculated using the Arrhenius equation. The bracketed values correspond to uncertainties.

R	Name	$k_{298\,K}$	E_a (kJ mol^{-1})	A (10^{16} s^{-1})	Ref.
$C_2H_5OC(O)$	PEFN	1.4×10^{-3}	108 (5)	1.2	This work
$C_2H_5C(O)$	PPN	3.5×10^{-4}	116 (2)	7.2	[5]
$CH_3OC(O)$	PMN	8.4×10^{-4}	107 (5)	0.48	[5]
$CH_3C(O)$	PAN	4.0×10^{-4}	113 (2)	2.5	[5]

E_a = Activation energy.
A = Pre-exponential factor.

As it can be seen in Table 5, the parameters obtained are similar to those reported for other peroxyacyl nitrates ($RC(O)OONO_2$). It is worth mentioning that:

a) PEFN stability is lower than that for PPN, probably due to the inclusion of an oxygen atom in the molecule, which decreases the activation energy. This can be explained on account of the electron withdrawal effect of the oxygen atom, which weakens the OO–N bond, making it less thermally stable (rows 1 and 2). A similar trend is observed between PMN and PAN (rows 3 and 4).
b) The rate constants of thermal decomposition are functions of the alkyl group, as it can be seen from the comparison between PEFN and PMN (rows 1 and 3), and between PPN and PAN (rows 2 and 4).

5.1. Photochemical and thermal lifetimes. Atmospheric implications

The loss of peroxynitrates in the atmosphere occurs through different processes, namely thermal decomposition, photolysis, and reaction with OH radicals. The relative importance of each of them depends on the region of the atmosphere and the structure of the molecule [30].

Fig. 5 depicts the thermal and photochemical lifetime profiles of PEFN as a function of altitude and latitude. The reciprocal of k_{-3} gives the thermal lifetime. This has been calculated from the kinetic parameters presented in Table 5 assuming, for temperatures lower than 279 K, the same activation energy as for the measured range.

Photochemical lifetimes were calculated using the TUV 4.2 program [31] as a function of altitude and solar zenith angle (SZA). A

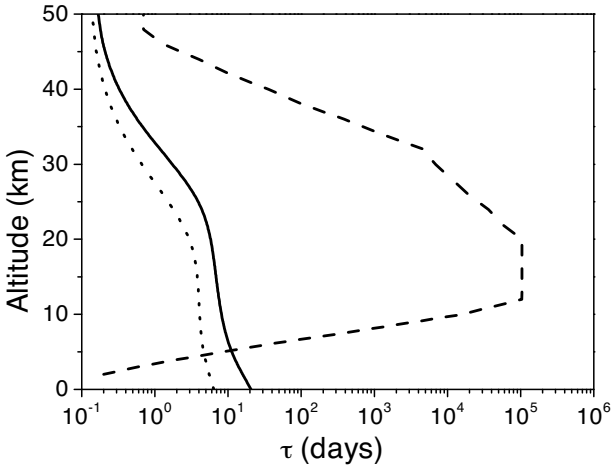

Fig. 5. Photochemical (dot and solid lines, for SZA of 0° and 60°, respectively), and thermal (dashed line) lifetimes of PEFN, as a function of altitude.

pressure independent quantum yield of unity at all wavelengths was assumed to run the TUV program since experimental values have not been reported to date. Taking into account that experimental data for the UV absorption cross-sections were determined up to 314 nm, we estimated the values corresponding to longer wavelengths by extrapolation with an exponential function to consider the photolysis of this molecule at longer wavelengths (lower altitudes). Photochemical lifetimes are the result of the diurnal average corresponding to the Southern Hemisphere equinox (21st September). Clear sky conditions were assumed.

As it can be observed in Fig. 5, the thermal lifetime behaves with altitude as expected according to the changes in the thermal profile of the atmosphere. In the troposphere, it lengthens substantially with altitude and ranges from 3 days at 5 km to one year in the vicinity of the tropopause, being slightly shorter than the one corresponding to PAN (4 days at 5 km [32]). As for PAN and other peroxynitrate analogues, the thermal decomposition of PEFN is a major loss process in the lower troposphere.

The photochemical lifetime at 0° and 60° is longer than the thermal lifetime in the surface and up to approximately 5 km, where the photochemical mechanism takes over. The increase in cross-sections as well as solar flux with altitude leads to an increase in the rate of photolysis and a consequent decrease in lifetime. Beyond the tropopause, the photochemical lifetime is of the order of a few hours, in agreement with the results for other similar molecules [33]. The figure also shows the photochemical lifetime to be shorter at 0° than at 60° as a result of higher solar radiation levels at the equator.

Although the rate constant for the reaction of OH with PEFN is unknown, it could be assumed to be similar to that corresponding to PAN ($k_{OH} < 3 \times 10^{-14}$ cm^3 molecule^{-1} [32]). Considering that: loss of PAN due to reaction of OH is very small throughout the entire troposphere; the reaction of PAN with OH is too slow to be competitive with thermal decomposition [32]; and that PAN and PEFN have similar thermal stabilities, we believe that the reaction of OH + PEFN should be too slow to compete with its thermal decomposition in the troposphere. Beyond the troposphere, no other channel can compete with the photochemical decomposition, and therefore all the other processes could be neglected.

Acknowledgments

Financial support from SECYT-UNC, ANPCyT and CONICET is gratefully acknowledged. The authors acknowledge use of the TUV program.

References

[1] F. Kirchner, L.P. Thuener, I. Barnes, K.H. Becker, B. Donner, F. Zabel, Environ. Sci. Technol. 31 (1997) 1801.
[2] S. von Ahsen, P. Garcia, H. Willner, G.A. Argüello, Inorg. Chem. 44 (2005) 5713.
[3] J.M. Roberts, Atmos. Environ. 24A (1990) 243.
[4] M. Manetti, F.E. Malanca, G.A. Argüello, Int. J. Chem. Kinet. 40 (2008) 831.
[5] F. Kirchner, A. Mayer-Figge, F. Zabel, K.H. Becker, Int. J. Chem. Kinet. 31 (1999) 127.
[6] A.P. Altshuller, J. Air Waste Manage. Assoc. 43 (1993) 1221.
[7] R. Atkinson, S.M. Aschmann, J.N. Pitts, J. Phys. Chem. A 92 (1984) 3454.
[8] S. Glavas, N. Moschonas, Atmos. Environ. 35 (2001) 5467.
[9] H.B. Singh, Environ. Sci. Technol. 21 (1987) 320.
[10] F. Caralp, V. Foucher, R. Lesclaux, T.J. Wallington, M.D. Hurley, Phys Chem Chem Phys 1 (1999) 3509.
[11] M.H. Harwood, J.M. Roberts, G.J. Frost, A.R. Ravishankara, J.B. Burkholder, J. Phys. Chem. A 107 (2003) 1148.
[12] G.S. Tyndall, R.A. Cox, C. Granier, R. Lesclaux, G.K. Moortgat, M.J. Pilling, A.R. Ravishankara, T.J. Wallington, J. Geophys. Res. Atmos. 106 (2001) 12157.
[13] F.E. Malanca, J.C. Fraire, G.A. Argüello, J. Photochem. Photobiol. A 204 (2009) 75.
[14] M.P. Sulbaek Andersen, O.J. Nielsen, M.D. Hurley, J.C. Ball, T.J. Wallington, D.A. Ellis, J.W. Martin, S.A. Mabury, J. Phys. Chem. A 109 (2005) 1849.
[15] M.P. Sulbaek Andersen, M.D. Hurley, T.J. Wallington, J.C. Ball, J.W. Martin, D.A. Ellis, S.A. Mabury, O.J. Nielsen, Chem. Phys. Lett. 379 (2003) 28.
[16] F.E. Malanca, M.D. Manetti, M.S. Chiappero, P. Gallay, G.A. Argüello, J. Photochem. Photobiol. A 205 (2009) 44.
[17] R. Kopitzky, H. Willner, H.G. Mack, A. Pfeiffer, H. Oberhammer, Inorg. Chem. 37 (1998) 6208.
[18] R. Kopitzky, M. Beuleke, G. Balzer, H. Willner, Inorg. Chem. 36 (1997) 1994.
[19] F. Zabel, F. Kirchner, K.H. Becker, Int. J. Chem. Kinet. 26 (1994) 827.
[20] D. Scheffler, I. Schaper, H. Willner, H.-G. Mack, H. Oberhammer, Inorg. Chem. 36 (1997) 339.
[21] P.W. Bruckmann, H. Willner, Environ. Sci. Technol. 17 (1983) 352.
[22] M.J. Frisch, G.W. Trucks, H.B. Schlegel, G.E. Scuseria, M.A. Robb, J.R. Cheeseman, V.G. Zakrzewski, J.A. Montgomery Jr., R.E. Stratmann, J.C. Burant, S. Dapprich, J.M. Millam, A.D. Daniels, K.N. Kudin, M.C. Strain, O. Farkas, J. Tomasi, V. Barone, M. Cossi, R. Cammi, B. Mennucci, C. Pomelli, C. Adamo, S. Clifford, J. Ochterski, G.A. Petersson, P.Y. Ayala, Q. Cui, K. Morokuma, D.K. Malick, A.D. Rabuck, K. Raghavachari, J.B. Foresman, J. Cioslowski, J.V. Ortiz, A.G. Baboul, B.B. Stefanov, G. Liu, A. Liashenko, P. Piskorz, I. Komaromi, R. Gomperts, R.L. Martin, D.J. Fox, T. Keith, M.A. Al-Laham, C.Y. Peng, A. Nanayakkara, C. Gonzalez, M. Challacombe, P.M.W. Gill, B. Johnson, W. Chen, M.W. Wong, J.L. Andres, C. Gonzalez, M. Head-Gordon, E.S. Replogle, J.A. Pople, Gaussian 98, Revision A.7, Gaussian, Inc., Pittsburgh, PA, 1998.
[23] O.N. Ventura, M. Kieninger, Chem. Phys. Lett. 254 (1995) 488.
[24] K. Raghavachari, B. Zhang, J.A. Pople, B.G. Johnson, P.M.W. Gill, Chem. Phys. Lett. 220 (1994) 1994.
[25] B.G. Johnson, C.A. Gonzalez, P.M.W. Gill, J.A. Pople, Chem. Phys. Lett. 221 (1994) 100.
[26] M.P. Badenes, J.C. Cobos, Theochem 856 (2008) 59.
[27] M.A. Burgos Paci, G.A. Argüello, P. García, F.E. Malanca, H. Willner, Inorg. Chem. 42 (2003) 2131.
[28] G. Allen, J.J. Remedios, D.A. Newnham, K.M. Smith, P.S. Monks, Atmos. Chem. Phys. 5 (2005) 47.
[29] E. Monedero, M.S. Salgado, F. Villanueva, P. Martín, I. Barnes, B. Cabañas, Chem. Phys. Lett. 465 (2008) 207.
[30] J.M. Roberts, PAN and related compounds, in: R. Koppmann (Ed.), Volatic Organic Compounds in the Atmosphere, Blackwell Publishing Ltd., Germany, 2007, pp. 221–268.
[31] S. Madronich, S. Flocke, The role of solar radiation in atmospheric chemistry, in: P. Boule (Ed.), Handbook of Environmental Chemistry, Springer, Heidelberg, 1998, p. 1.
[32] R.K. Talukdar, J.B. Burkholder, A.M. Schmoltner, J.M. Roberts, R.R. Wilson, A.R. Ravishankara, J. Geophys. Res. 100 (1995) 14163.
[33] F.E. Malanca, M.S. Chiappero, G.A. Argüello, J. Photochem. Photobiol. A 184 (2006) 212.